Original Article

Regional delivery of mesothelin-targeted chimeric antigen receptor T-cell effectively and safely targets colorectal cancer liver metastases in mice

Xin Zhou[1,2,3#], Minjie Yang[1,2,3#], Jiaze Yu[1,2,3], Jingwen Tan[4], Nan Xu[4], Yongjie Zhou[1,2,3], Wen Zhang[1,2,3], Jingqin Ma[1,2,3], Zihan Zhang[1,2,3], Alex Friedlaender[5], Justin Taylor[6], Lei Yu[4], Zhiping Yan[1,2,3]^

[1]Department of Interventional Radiology, Zhongshan Hospital, Fudan University, Shanghai, China; [2]Shanghai Institution of Medical Imaging, Shanghai, China; [3]National Clinical Research Center for Interventional Medicine, Zhongshan Hospital, Fudan University, Shanghai, China; [4]Shanghai Unicar-Therapy Bio-Medicine Technology Co., Ltd., Shanghai, China; [5]Department of Oncology, Clinique Générale Beaulieu, Geneva, Switzerland; [6]Department of Medicine, Sylvester Comprehensive Cancer Center, University of Miami Miller School of Medicine, Miami, FL, USA

Contributions: (I) Conception and design: Z Yan, L Yu; (II) Administrative support: J Yu, J Tan; (III) Provision of study materials or patients: N Xu, Y Zhou, W Zhang, J Ma; (IV) Collection and assembly of data: X Zhou; (V) Data analysis and interpretation: X Zhou, M Yang; (VI) Manuscript writing: All authors; (VII) Final approval of manuscript: All authors.

[#]These authors contributed equally to this work

Correspondence to: Zhiping Yan, MD. Department of Interventional Radiology, Zhongshan Hospital, Fudan University, No. 180 Fenglin Road, Xuhui District, Shanghai 200032, China; Shanghai Institution of Medical Imaging, Shanghai, China; National Clinical Research Center for Interventional Medicine, Zhongshan Hospital, Fudan University, Shanghai, China. Email: yan.zhiping@zs-hospital.sh.cn; Lei Yu, PhD. Shanghai Unicar-Therapy Bio-medicine Technology Co., Ltd., No. 1525 Minqiang Road, Shanghai 201612, China. Email: ylyh188@163.com.

Background: Liver metastasis is the major cause of colorectal cancer related death. Mesothelin (MSLN)-targeted chimeric antigen receptor (CAR) T-cell therapy has been illustrated effective and safe through regional delivery of breast cancer, ovarian cancer and malignant mesothelioma tumors. Herein, we investigated the safety, efficacy, and immune microenvironment of regional delivery of MSLN (CAR) T-cell in the treatment of colorectal carcinoma liver metastases (CRLM).

Methods: Second-generation MSLN CAR T-cells were administered by portal vein (PV) or caudal vein (CV, systemic administration) delivery in an orthotopic MSLN$^+$ CRLM nonobese diabetic (NOD)/severe combined immunodeficient (SCID)/$\gamma c^{-/-}$ (NSG) mouse model. A total of 20 mice were randomly divided into control group, non-transduced T cell (NT)-CV group, NT-PV group, MSLN CAR T-cell CV (MSLN-CV) group, and MSLN CAR T-cell PV (MSLN-PV) group, with each group containing four mice to examine the safety and efficacy. The bioluminescence intensity (BLI) of tumor burden, tumor tissue macroscopic and microscopic observation were used to evaluate treatment efficacy. The safety was examined by body weight, survival time, and vital organ damage of mice. CAR T-cell infiltration and cytokine concentration were analyzed by flow cytometry, and immunostaining. The change of immune microenvironment between regional delivery and systemic delivery was investigated on an immune reconstructed CRLM patient-derived xenograft (PDX) model. Additionally, T cell subsets and immunosuppressive markers were examined.

Results: PV administration of 1×10^7/100 μL MSLN CAR T-cells in 20 NSG mice was well tolerated, and no overt toxicity was observed. The tumor burden in the PV group was obviously alleviated. The BLI was $(0.73\pm0.52)\times10^9$ in PV group and $(1.97\pm0.11)\times10^9$ in CV group ($P<0.05$), CD8$^+$ granzyme B (GB)$^+$ T cell percentage (MSLN-CV 4.42%±0.47% *vs.* MSLN-PV 13.5%±4.67%, $P<0.01$) and cytokine concentration were obviously increased in the MSLN-PV group. In the immune reconstituted CRLM PDX model, intratumor (IT) delivery of MSLN CAR T-cells exhibited much more infiltration of CD4$^+$ and CD8$^+$ T cells accompanied with elevated expression levels of PD-1, LAG-3, and TIM-3.

^ ORCID: 0000-0002-4012-4572.

Conclusions: Regional delivery of MSLN-targeted CAR T-cell therapy has encouraging results in the orthotopic CRLM NSG mouse model and PDX model, and converts the tumor microenvironment from cold to hot. This study may provide a new therapeutic approach for CRLM. Further clinical study is needed.

Keywords: Regional delivery; mesothelin (MSLN); chimeric antigen receptor T-cell (CAR T-cell); colorectal carcinoma liver metastases (CRLM)

Submitted Jan 10, 2024. Accepted for publication Feb 16, 2024. Published online Feb 28 2024.
doi: 10.21037/jgo-24-25
View this article at: https://dx.doi.org/10.21037/jgo-24-25

Introduction

Liver metastases are one of the reasons for the high mortality of colorectal carcinoma. They are associated with poor therapeutic response, further limited by the remaining normal liver volume and liver function (1). Despite significant advances in treatment strategies in recent decades (2,3), the efficacy of treatments and prognosis of colorectal carcinoma liver metastases (CRLM) are still suboptimal. Therefore, new therapies for CRLM are urgently needed.

Liver immune microenvironment has an influence on the therapeutic effect. As the immunosuppressive characteristics of the liver promote the development of CRLM, delivery of specific T cells to treat CRLM is a rational strategy. Chimeric antigen receptor (CAR) T-cell therapy has already demonstrated promising results in hematologic malignancies (4), while CAR T-cells combined with immune checkpoint inhibitors enhance antitumor efficacy in malignant pleural mesothelioma (5). CRLM may be treatable with CAR-based immunotherapy. Mesothelin (MSLN), which has been used as a therapeutic target for monoclonal antibodies, immunotoxins, and vaccines (6-8), is an attractive CAR target due to its high expression in a number of digestive solid tumors, very low expression in mesothelial cells, and its association with invasion and the development of metastases (9-12).

However, the published literature of the therapeutic effect of CAR T-cells in solid tumors shows their efficacy is unfortunately impeded by T cell homing and infiltration into the tumor (13). Regional delivery of CAR T-cells, such as intrapleural, intracranial, and intraperitoneal administration has demonstrated superior antitumor response and safety compared to systemic administration (14-16). To address these obstacles, we established a clinically relevant CRLM orthotopic mouse model, and a patient-derived xenograft (PDX), which is extremely mimic CRLM patients' tumor condition and microenvironment, to examine whether MSLN CAR T-cell could eradicate CRLM and to study the stimulation of the immune microenvironment after regional delivery of CAR T-cells, providing experimental data for further clinical trials. We present this article in accordance with the ARRIVE reporting checklist (available at https://jgo.amegroups.com/article/view/10.21037/jgo-24-25/rc).

Highlight box

Key findings

- Regional delivery of mesothelin (MSLN)-targeted chimeric antigen receptor (CAR) T-cell effectively controls tumor growth of colorectal carcinoma liver metastases (CRLM) in a mouse model and converts cold tumors into hot tumors.

What is known and what is new?

- MSLN CAR T-cell has been demonstrated effective antitumor response in several solid tumors.
- The regional administration of CAR T-cell is more effective and safer than systemic delivery. Portal vein delivery of MSLN CAR T-cell significantly suppresses CRLM progress, and enhances cytotoxic T cell infiltration and tumor cell killing.

What is the implication, and what should change now?

- This might provide a promising therapy for CRLM.

Methods

Study design

The objective of this study was to assess CAR T-cell immunotherapy for CRLM. We developed a fully human second-generation MSLN CAR T-cell. In this study, we selected three delivery routes for MSLN CAR T-cell, including portal vein (PV), intratumor (IT), and systemic administration. *In vitro*, we analyzed MSLN CAR T-cell (I) transduction efficiency and (II) cytotoxicity. *In vivo*, we first established an orthotopic MSLN$^+$ CRLM nonobese diabetic

(NOD)/severe combined immunodeficient (SCID)/$\gamma c^{-/-}$ (NSG) mouse model to examine antitumor efficacy and safety after MSLN CAR T-cell administration. In this part, 20 NSG mice (sourced from Shanghai Model Organisms, Shanghai, China) were randomly divided into a control group, non-transduced T cell (NT)-caudal vein (CV) group, NT-PV group, MSLN CAR T-cell CV (MSLN-CV) group, and MSLN CAR T-cell PV (MSLN-PV) group, with each group containing four mice. In order to mimic the immune microenvironment in humans, we developed a humanized immune reconstituted percutaneous CRLM PDX model, from which nine NSG tumor bearing mice were randomly divided into a control group, CV group, and IT group to explore the change of immune microenvironment between regional delivery and systemic delivery of MSLN CAR-T cell. The experimental procedures were approved by the Institutional Animal Care and Use Committee of Zhongshan Hospital, Fudan University (No. B2020-009R2) and institutional guidelines for the care and use of animals were followed. A protocol was prepared before the study without registration. All NSG mice were fed and housed under specific-pathogen-free conditions.

Cell lines

Human colorectal carcinoma cell line (HCT-8), human pancreatic tumor cell lines (PANC-1, ASPC-1, and BXPC-3), human gastric tumor cell line (HGC-27), K562, MSLN-K562, and H-MSLN-Luc-HCT-8, Raji cell line were incubated in Roswell Park Memorial Institute (RPMI) 1640 containing 10% fetal bovine serum (FBS). The human fibrosarcoma kidney cell line 293T was cultured in Dulbecco's modified Eagle medium (DMEM) containing 10% FBS. We first established the MSLN-overexpressed cell line H-MSLN-Luc-HCT-8. The expression of MSLN and luciferase in the established cell line was verified by western blot (WB) and luciferase examination. All cells were cultured at 37 ℃ with 5% CO_2. MSLN-K562, H-MSLN-Luc-HCT-8, and Raji cell line were supplied by Shanghai Unicar-Therapy Bio-medicine Technology Co., Ltd. (Shanghai, China), other cells were obtained from the Cell Bank of the Chinese Academy of Sciences (Shanghai, China).

Human CAR T-cell production

The MSLN CAR construct is a fully human second-generation vector, including the following components in-frame from the 5' end to the 3' end: anti-MSLN single-chain variable fragment (scFv), the hinge and transmembrane domain of the CD8α molecule, 4-1BB co-stimulatory domain (17), and the CD3 zeta intracellular signaling domain (*Figure 1A*). The CD19 CAR was prepared as the control group, and had the same structure, except for anti-CD19 scFv. Lentiviruses were generated from these constructs via transient transfection of HEK293T cells. Peripheral blood mononuclear cells (PBMCs) of healthy donors were isolated by gradient centrifugation using mononuclear cell isolation fluid (Oriental Hua Hui, Beijing, China) followed by $CD4^+$ T-cell and $CD8^+$ T-cell positive selection by a magnetic bead separation method (Miltenyi Biotec, Bergisch Gladbach, Germany). $CD4^+$ and $CD8^+$ T cells were co-cultured and activated using anti-CD3/CD28 monoclonal antibodies (Miltenyi Biotec) in a 37 ℃, 5% CO_2 temperature incubator *in vitro* for 24 hours, and then transduced with lentivirus (MSLN CAR and CD19 CAR) for 48 hours. After transduction, the CAR T-cells were cultured and expanded in AIM-V medium with interleukin (IL)-2 cytokine (Gibco, Grand Island, NY, USA).

Cytotoxicity assays

Quantitation of lactate dehydrogenase (LDH) activity (18) was examined to test the cytotoxicity of CAR T-cell from the effector and target cell co-cultured supernatants using the cytotoxicity detection kit (Promega, Madison, WI, USA). All the MSLN or CD19 CAR T-cells as effector cells (E) were co-cultured with the overexpressed CD19 or MSLN target cells (T) at E:T ratios of 10:1, 5:1, and 2.5:1, respectively. Effector and target cells were inoculated with a total of 100 μL with serum-free RPMI 1640 media (Gibco) in 96-well plates and cultured at 37 ℃ for 24 hours. After co-culture, 50 μL of cell-free supernatant from each well was harvested and mixed with equal volume of LDH substrate mixture and seeded in new 96-well plates, after 15 minutes of incubation in the dark at 25 ℃. The absorbance was detected at 490 nm using a full wavelength enzyme labeling instrument (Multiskan GO; Thermo Fisher Scientific, Waltham, MA, USA). Cytotoxicity (%) = (experimental LDH release – spontaneous LDH release)/(maximum LDH release – spontaneous LDH release) × 100%.

Expression of CD107A

CD107A is an indirect marker of degranulation of T cells. To examine CD107A expression level, 1×10^5 CAR T-cells and target cells with a total volume of 200 μL of AIM-V

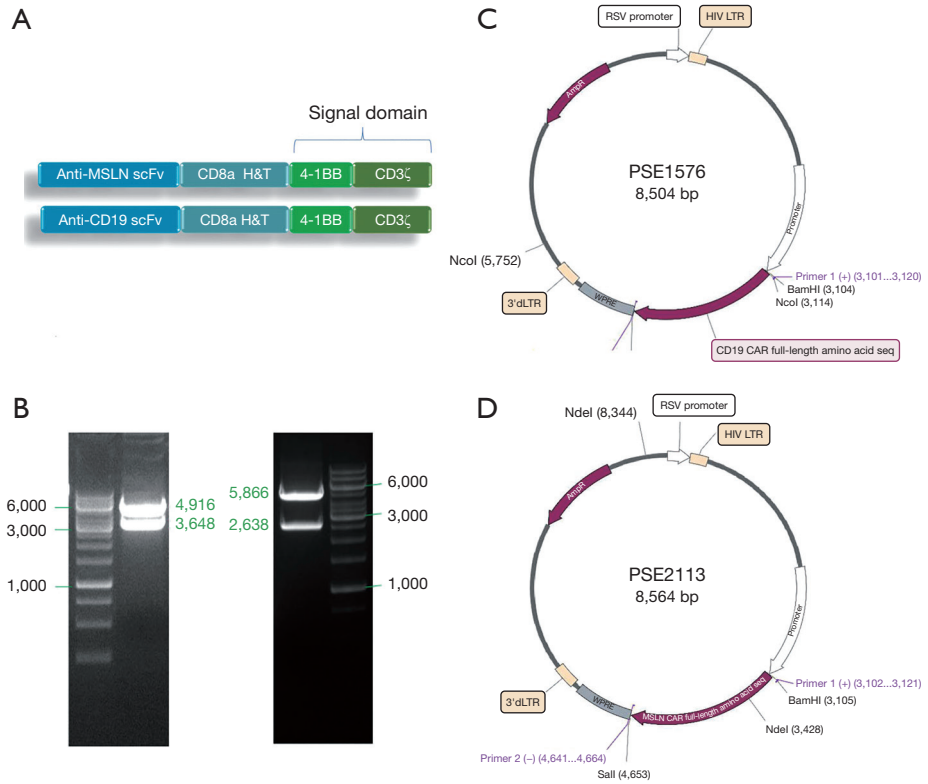

Figure 1 CAR design and generation characterization. (A) Structure schematic diagram of second-generation of MSLN CAR and CD19 CAR; (B) gel electrophoresis of PSE2113 (left) PES1576 (right); (C) schematic diagram of target plasmid PSE1576; (D) schematic diagram of target plasmid PSE2113. MSLN, mesothelin; scFv, single-chain fragment variable; H&T, hinge & transmembrane region; RSV, Rous sarcoma virus; HIV, human immunodeficiency virus; LTR, long terminal repeat; dLTR, defective LTR; WPRE, woodchuck hepatitis post-transcriptional regulatory element; CAR, chimeric antigen receptor.

medium (Gibco) were co-cultured at a ratio of 5:1 in 96-well plates for 6 hours. Before the incubation, the Golgi inhibitor monensin (Invitrogen, Carlsbad, CA, USA) was added. In the positive control group, cocktails (Invitrogen) were added. After a 6-hour incubation, cells were labeled with CD107A, CD3, and CD8 monoclonal antibodies for flow cytometry. FlowJo 10 software [Becton, Dickinson and Co. (BD) Biosciences, Franklin Lakes, NJ, USA] was used for results analysis.

T-cell activation assay

Flow cytometry for CD69, CD25, and CD279 expression was performed to evaluate T-cell activation. NT were selected as negative controls. After 24 hours of co-culture with target cells, the cells were harvested and labeled with CD69, CD25, CD279, CD3, and protein L monoclonal antibodies for 45 minutes at 4 ℃ in the dark.

Mouse orthotopic CRLM model

Female NSG mice between 6 and 8 weeks old were used for orthotopic CRLM establishment. Mice were anesthetized under inhaled isoflurane analgesia. An oblique incision was made in the left upper abdomen, and 1.0×10^6 or 2.5×10^6 H-MSLN-Luc-HCT-8 cells in 50 µL 0.9% sodium chloride injection were injected into the spleen; after 15 minutes, the spleen was cut to ensure more tumor cells colonize the liver. The CRLM were monitored by IVIS Lumina III (PerkinElmer, Waltham, MA, USA). In total, 1×10^7 MSLN CAR T-cells/NT T-cells were injected into tumor-bearing mice with 100 µL of 0.9% sodium chloride, through PV delivery or systemically by CV delivery. The liver was harvested to examine the tumor burden, and the heart, lung, kidney, and pancreas were obtained to estimate the vital organ damage. Peripheral blood was obtained by retro-orbital bleeding.

Immune reconstructed CRLM PDX model

To mimic the human immune microenvironment, a MSLN$^+$ CRLM PDX model confirmed by immunohistochemistry (IHC) was developed. First, the CRLM tissue was sliced into pieces 2 mm × 2 mm × 2 mm in size and injected into percutaneous tissue of female 6–8-week-old NSG mice. The tumor was measured once a week by vernier caliper. When the largest diameter was 10 mm, 5×10^6 human (hu)PBMC were injected through CV. Peripheral blood was obtained by retro-orbital bleeding to test huCD3$^+$ T cell and huCD45$^+$ T cell by flow cytometry. When the huCD45$^+$ T cells percentage was >50% and huCD3$^+$ T cells percentage was >90%, the immune status was deemed to have been reconstructed successfully. When the tumor volume reached 500 mm^3, 1×10^7 MSLN CAR T-cells were injected by IT injection or CV.

Histologic analysis and immunostaining

Histopathologic evaluation of the tumor tissues and vital organs was performed via hematoxylin and eosin (HE) staining. IHC analysis for human MSLN, CD8, and granzyme B (GB) was performed of the mice tumor tissue.

Safety evaluation in vivo

Body weight, survival time and vital organ damage were selected to evaluate safety index. Body weight of mice was measured twice a week. When weight loss exceeds 30%, the mice were euthanized. Survival time of each group was recorded. Vital organ damage was assessed by the result of HE staining.

Efficacy evaluation in vivo

Tumor burden of orthotopic CRLM model was monitored by living imaging, macroscopic and microscopic observation. Tumor size of PDX model were measured by vernier calipers. Tumor volume was calculated by the formula: 0.5 × length × width^2.

Correlative studies

We performed flow cytometry using human monoclonal antibodies MSLN, CD3, CD4, CD8, GB, CD127, and CD25 in mice peripheral blood and tumor tissue. The human LAG-3, TIM-3, and PD-1 levels of tumor tissue in the PDX model were confirmed by IHC and the expression amounts were recorded. Cytokine release was evaluated using a cytometric bead array (CBA) human T helper (Th)1/Th2/Th17 CBA kit (BD Bioscience) according to the manufacturer's instructions. The cytokine detection assays were performed by flow cytometry using a Th1/Th2 CBA kit (BD Bioscience).

Statistical methods

Data were presented as mean ± standard deviation (SD). The difference between multiple groups was compared by one-way analysis of variance (ANOVA), and the difference in continuous variables between the two groups was analyzed by Student's *t*-test. $P<0.05$ indicated a statistically significant. The software GraphPad Prism 6 (GraphPad Software, San Diego, CA, USA) was used for graph generation and statistical analyses.

Results

MSLN CAR T-cells notably respond to MSLN$^+$ target cells

In this study, the second-generation MSLN CAR T-cells were successfully constructed (*Figure 1*). As shown in *Figure 2*, the transduction efficiency of MSLN CAR T-cells ranged from 15% to 24.9%. We detected gastric cancer HGC-27, colon cancer HCT-8, pancreatic cancer PANC-1, BXPC-3, and ASPC-1 cell lines for MSLN expression. K562 cell was used as the negative control group, and the MSLN-K562 cell line was detected at the same time. Among them, the MSLN-K562 stable strain had the highest MSLN expression, followed by HGC-27 and HCT-8 (*Figure 3*). Cytotoxicity analysis indicated that MSLN CAR T-cell effectively killed the MSLN-positive HCG-27 and HCT-8 cells, but had nearly no killing effect on non-expressing and low MSLN expressing K562, Raji, ASPC-1, and BXPC-3 cell lines (*Figure 4*). According to the purpose to study the treatment of CAR T-cell for CRLM and the results of MSLN antigen expression verification, HCT-8 was selected for follow-up study. As shown in *Figure 5*, MSLN CAR T-cells and CD19 CAR T-cells had killing function *in vitro* and were specific to target antigen killing, which enhanced with the increase of effect-target ratio in a dose-dependent manner. Furthermore, we tested CD107A as indirect marker to reflect CAR T-cell killing capacity; the degree of expression of CD107A of MSLN CAR T-cell increased when co-cultured with HCT-8 and K562-MSLN,

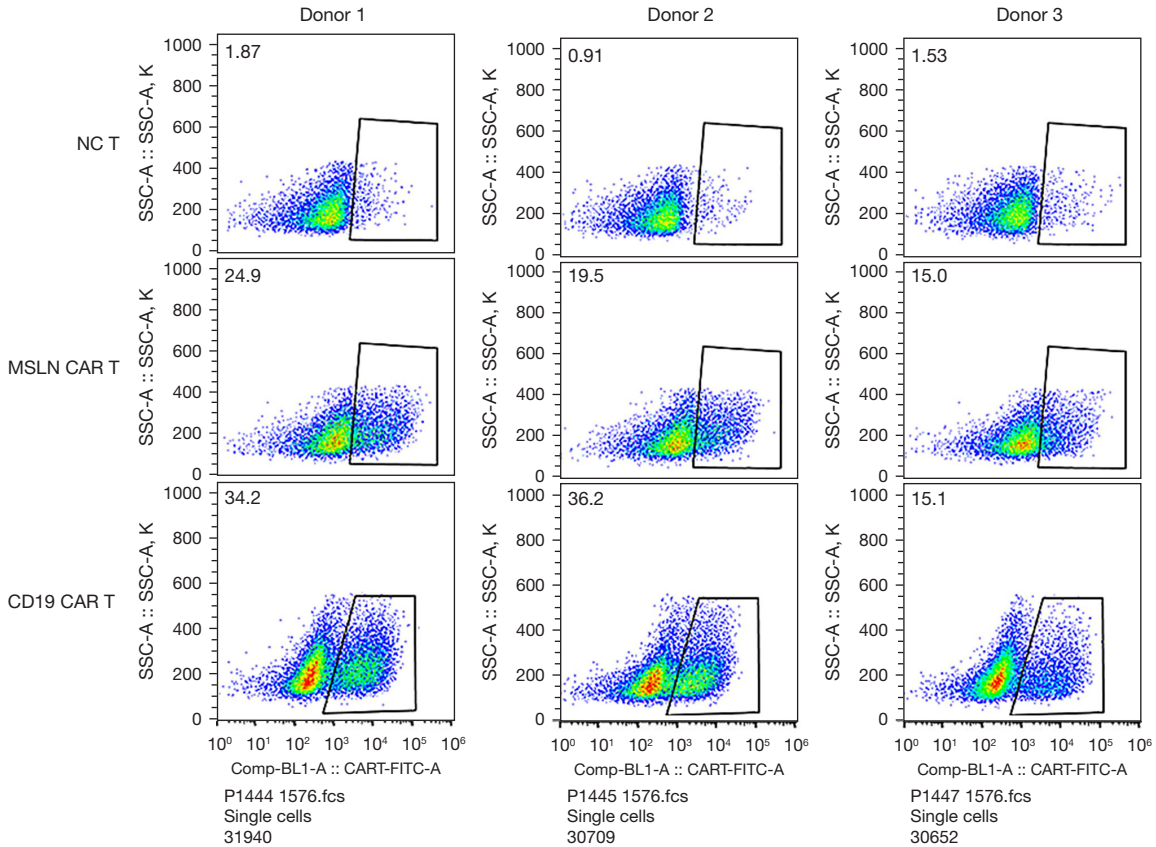

Figure 2 CAR transduction efficiency. NC, negative control; MSLN, mesothelin; CAR, chimeric antigen receptor; FITC, fluorescein isothiocyanate.

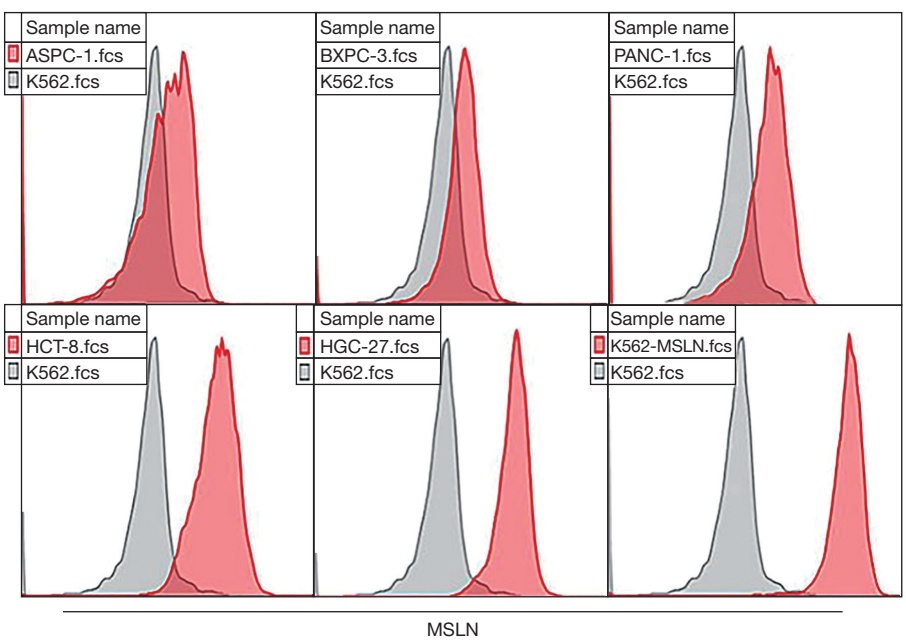

Figure 3 Tumor cell MSLN expression. MSLN, mesothelin.

indicating that the cytotoxic effect of MSLN CAR T-cell was specific to MSLN$^+$ target tumor cell (*Figure 6*). We further examined the T cell activation markers, and it was shown that the two target cells HCT-8 and K562-MSLN that express MSLN antigen can up-regulate the activation markers CD25, CD69, and PD-1 on CAR T-cells (*Figure 7*). It was shown that MSLN CAR T-cells are specifically activated by MSLN antigen, and the cytotoxic effect is conferred by the MSLN CAR gene.

Regional PV delivery of MSLN CAR T-cells is more effective to eradicate CRLM than the systemic route

Based on *in vitro* results, the HCT-8 cell line was selected for *in vivo* antitumor assays. We established an orthotopic CRLM NSG mouse model using the H-MSLN-HCT-8 cell line (*Figure 8*). After 12 days, mice were treated with NT-cells and MSLN CAR T-cells through PV or CV delivery, when the median bioluminescence intensity (BLI) of the tumor burden reached $(4.1\pm1.5)\times10^9$ (*Figure 9A*). Following a single dose, MSLN CAR T-cells/NT T-cells were administered by PV or CV delivery. It was found that tumor growth was controlled in both the MSLN-CV and MSLN-PV groups. On day 7, the BLI signal of CRLM decreased in the MSLN-PV group, and CRLM disappeared in two mice on day 21. The BLI signal decreased later in the MSLN-CV group until day 14 (*Figure 9B*). In the control group, NT-CV, and NT-PV groups, effective control of the tumor growth was not achieved and the mice died on day 14 (*Figure 9A*). The tumor load was confirmed by HE staining and visual observation (*Figure 9C,9D*); tumor burden was effectively controlled in the MSLN PV group. According to the results of body weight, fur condition, and vital organ, including heart, kidney, lung, and pancreas HE staining, the PV route appeared safe, without obvious toxicities (*Figure 10*).

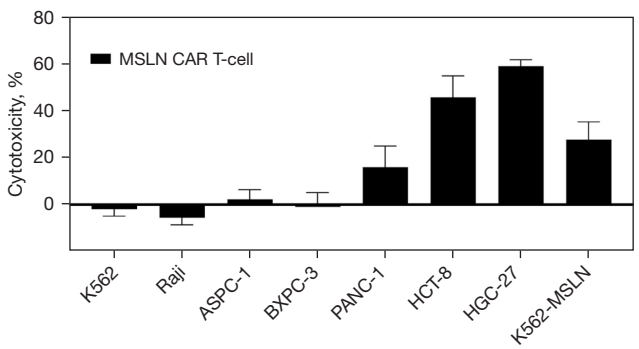

Figure 4 The killing efficiency of MSLN CAR T-cells against different intensity target antigen cells was detected. MSLN, mesothelin; CAR, chimeric antigen receptor.

PV delivery of MSLN CAR T-cell increases the T cell infiltration and homing in tumor

According to the CAR T-cell ineffective homing in solid tumors, we examined MSLN CAR T-cell in the liver for the MSLN CV and MSLN PV groups. As shown in *Figure 11A*, a significant increase in MSLN$^+$CD3$^+$ T cells was found in the PV group compared with the CV group (PV *vs.* CV, P<0.001). Further analysis of T cell subgroups showed that the CD4$^+$ T cell percentage was higher in the PV group compared with the CV group, and CD8$^+$GB$^+$ T cell percentage was increased in the MSLN-PV group on day 14 (MSLN-PV *vs.* MSLN-CV, P<0.01; *Figure 11B*). In addition, the infiltration of human CD8$^+$GB$^+$ T-cell was further verified by IHC analysis of CRLM tumors

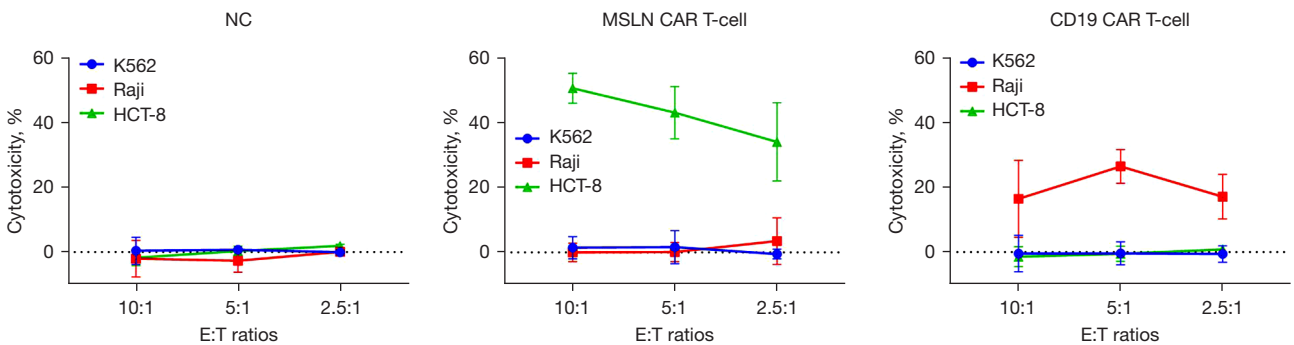

Figure 5 CAR T-cell killing capacity *in vitro*. NC, negative control; MSLN, mesothelin; CAR, chimeric antigen receptor; E:T, effect cell:target cell.

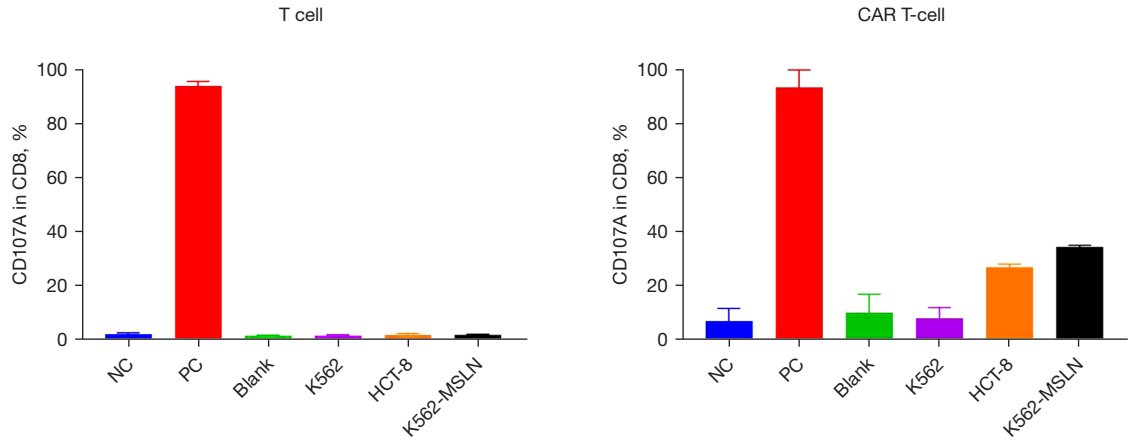

Figure 6 MSLN CAR T-cell degranulation effect verification. NC, negative control; PC, positive control; MSLN, mesothelin; CAR, chimeric antigen receptor.

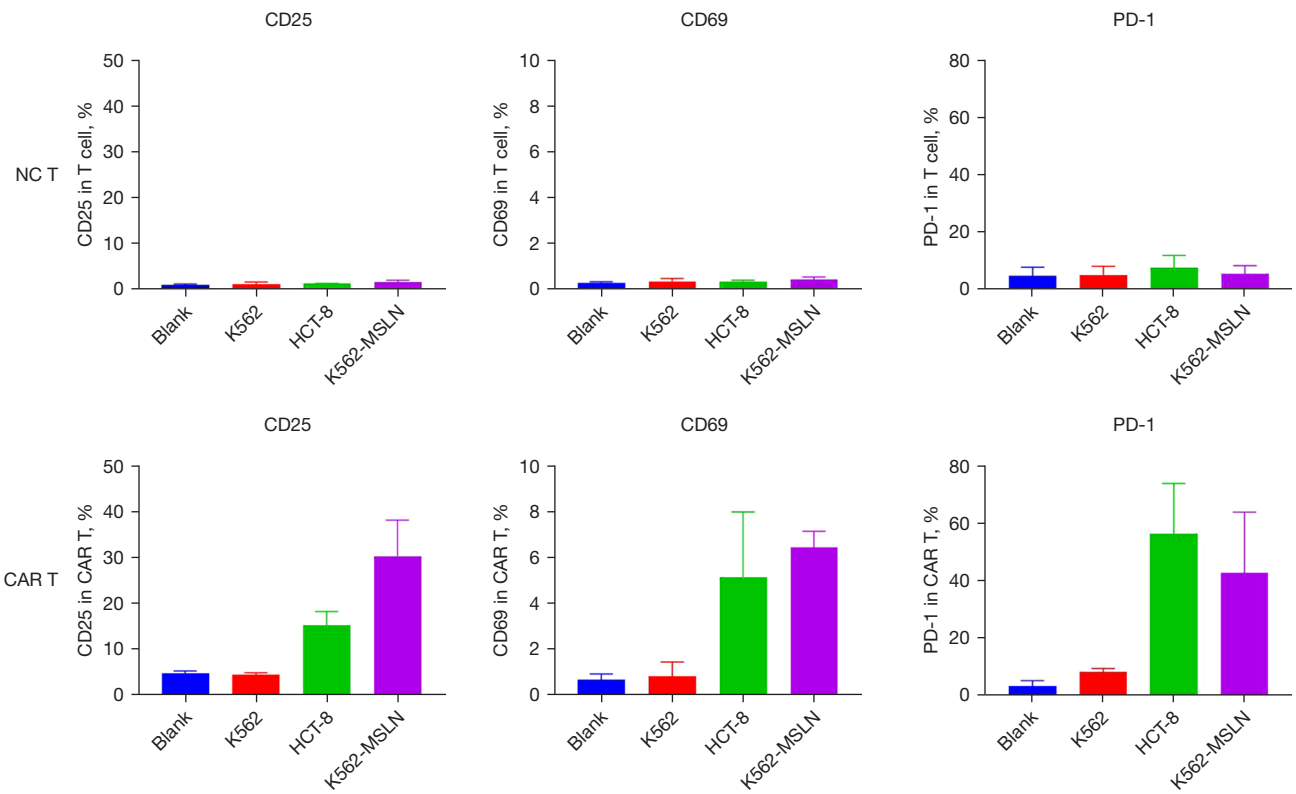

Figure 7 MSLN positive tumor cells specifically activated MSLN CAR T-cells. NC, negative control; MSLN, mesothelin; CAR, chimeric antigen receptor.

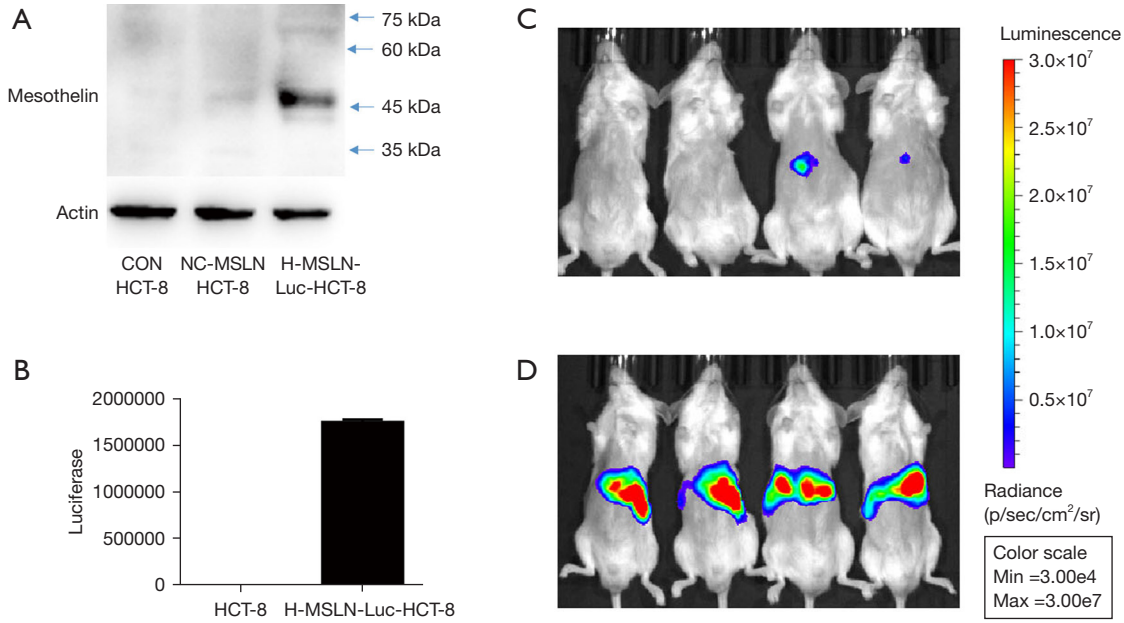

Figure 8 H-MSLN-Luc-HCT-8 cell line identification and CRLM mouse model establishment. (A) WB result of MSLN expression; (B) luciferase expression; (C) tumor establishment of 1×10^6 H-MSLN-Luc-HCT-8 cell; (D) tumor establishment of 2.5×10^6 H-MSLN-Luc-HCT-8 cell. CON, control; NC, negative control; MSLN, mesothelin; CRLM, colorectal carcinoma liver metastases; WB, western blot.

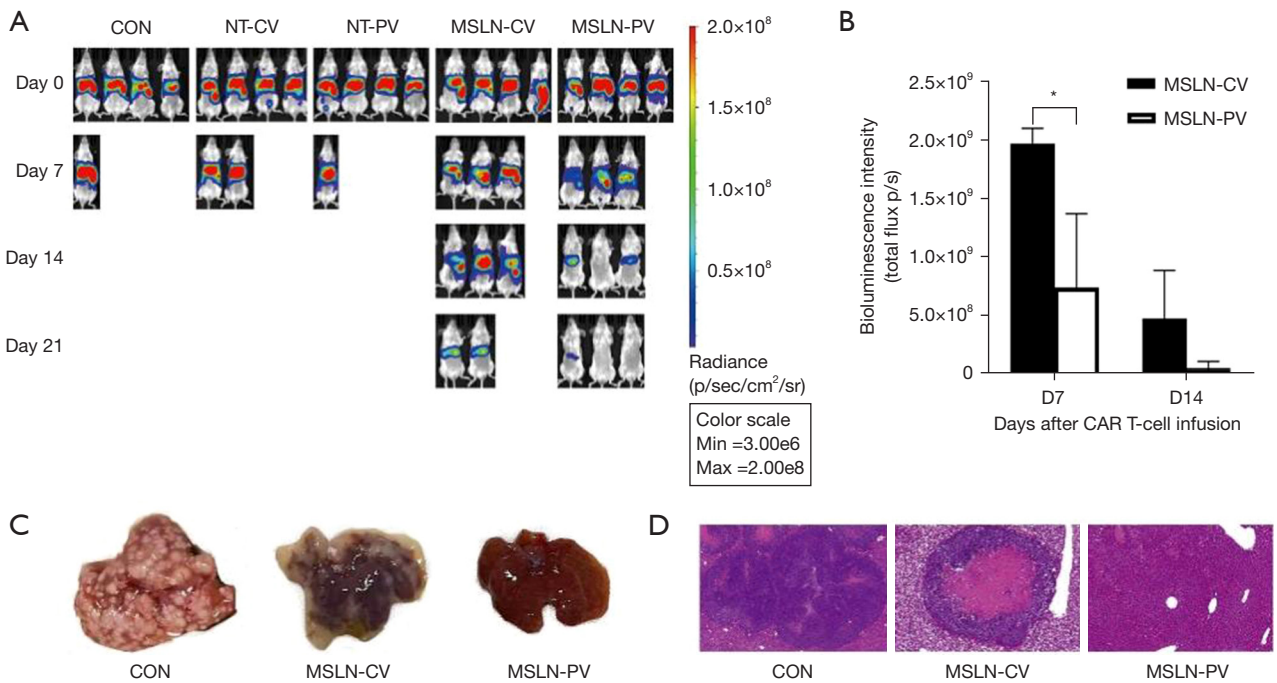

Figure 9 PV delivery of MSLN CAR T-cells effectively control CRLM growth in mouse orthotopic CRLM model. (A) Living imaging result; (B) the change of BLI in MSLN-CV and MSLN-PV group; (C) tumor gross observation; (D) tumor HE staining (4×). D0 is the time for CAR T-cell delivery. *, represents P<0.05. CON, control; NT, non-transduced T cell; CV, caudal vein; PV, portal vein; MSLN, mesothelin; CAR, chimeric antigen receptor; BLI, bioluminescence intensity; HE, hematoxylin and eosin.

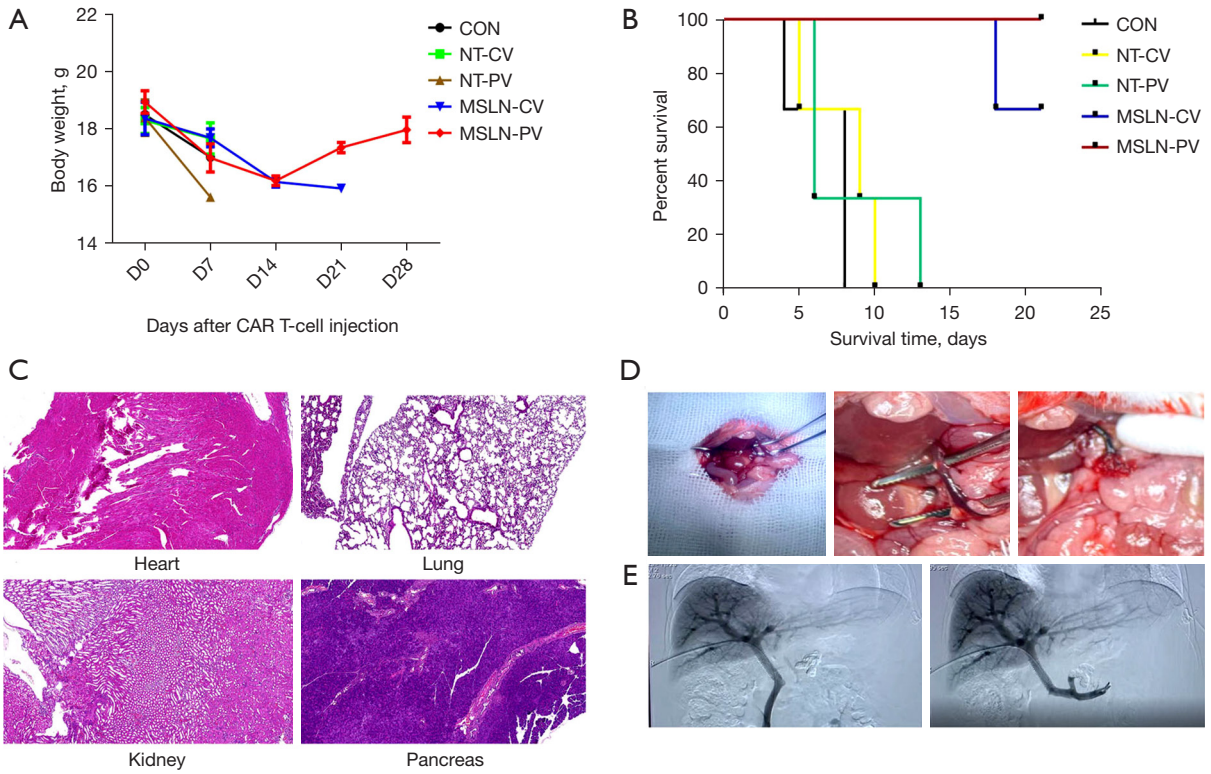

Figure 10 PV delivery of MSLN CAR T-cells don't cause obvious toxicity. (A) Body weight of NSG mice; (B) Survival curve of NSG mice; (C) Vital organ HE staining of PV group (heart, lung, kidney, and pancreas) (4×); (D) PV puncture of mice; (E) human PV angiography. CON, control; NT, non-transduced T cell; CV, caudal vein; PV, portal vein; MSLN, mesothelin; CAR, chimeric antigen receptor; NSG, NOD/SCID/$\gamma c^{-/-}$; NOD, nonobese diabetic; SCID, severe combined immunodeficient; HE, hematoxylin and eosin.

(*Figure 11C*). Previous study has shown that CAR T-cell therapy can lead to a whole-body immune response and the abscopal effect, which are hypothesized to be due to cytokine secretion (19). To explore cytokine secretion differences between different delivery routes of MSLN CAR T-cells, the major cytokines [interferon (IFN)-γ, IL-2, tumor necrosis factor (TNF)-α, IL-4, IL-6, IL-17A] which had a correlation with MSLN CAR T-cell function were analyzed. Higher levels of IL-2, IL-6, IFN-γ, and IL-17A were secreted in the PV group than in the CV group (*Figure 11D*). These cytokines could enhance the antitumor response of CAR T-cell and induce the whole-body immune response. PV delivery resulted in greater CAR T-cell proliferation, tumor eradication, and survival rate than systemic administration.

The immune status after local delivery of MSLN CAR T-cell in PDX model

Median MSLN expression in the CRLM was 56.3% (9/16) positive (*Figure 12A*). Due to the long period of PDX model construction (4–6 months), low survival rate of NSG mice undergoing laparotomy, harsh feeding conditions, and difficulties in monitoring intrahepatic PDX model, the PDX model of subcutaneous CRLM was constructed in this part (*Figure 12B*). The first- and second-generation PDX models were amplified, and nine mice of the second-generation PDX model were selected for follow-up experiments. When the tumor volumes reached 500 mm^3, human immune reconstructed models were developed. The percentage of human $CD45^+$ T cell reached 68.43%±16.44% and the $huCD3^+$ T cell percentage was 96.45%±16.44%, indicating that the immune reconstruction model had been successfully established (*Figure 13*). After that, mice were divided into three groups: the control group (the same dose of 0.9% sodium chloride as the other two groups), IT injection group, and CV injection group with a single dose of $1×10^7$ MSLN CAR T-cell. As shown in *Figure 14*, on day 21, the tumor volume was 119.66±66.1 mm^3 in the IT group, 294.29±75.64 mm^3 in the CV

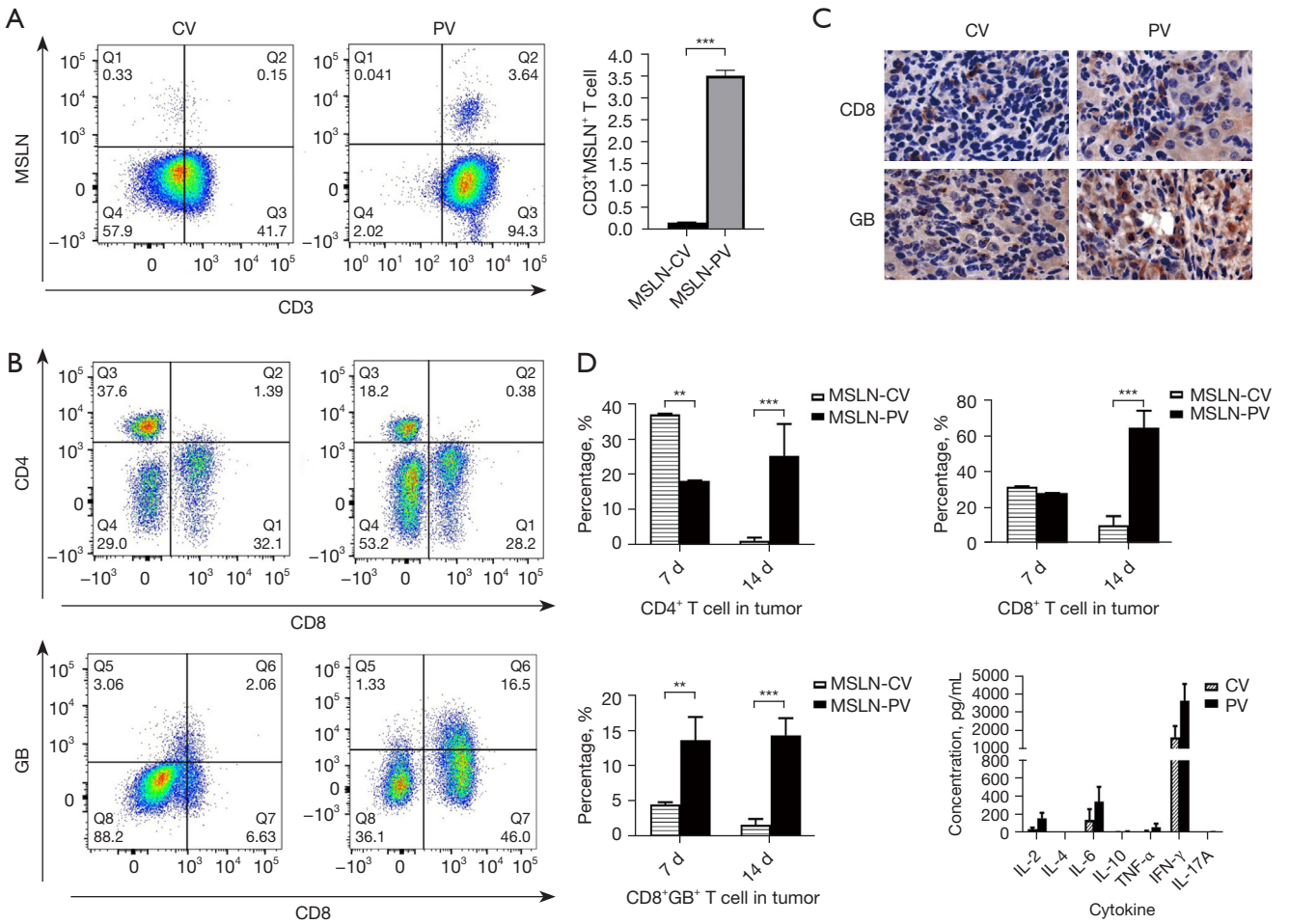

Figure 11 CAR T-cell distribution in tumor tissue and secretion of cytokines in peripheral blood. (A) MSLN CAR T-cell infiltration in tumor tissue between CV and PV groups; (B) the CD4$^+$ T cell and CD8$^+$ T cell in tumor tissue; (C) The IHC results of CD8 and GB positive staining (20×); (D) cytokine secretion in peripheral blood. **, represents P<0.01; ***, represents P<0.001. MSLN, mesothelin; CV, caudal vein; PV, portal vein; GB, granzyme B; IL, interleukin; TNF, tumor necrosis factor; IFN, interferon; CAR, chimeric antigen receptor; IHC, immunohistochemistry.

group, and 921.26±273.02 mm^3 in the control group. Due to the huPBMC model limit, the decrease of mice weight surpassed 30% (*Figure 14B*), or the GvHD effect appeared, the experiment was terminated. The tumor and peripheral blood were harvested to investigate the immune microenvironment of T cells after CAR T-cell treatment. As shown in *Figure 15*, a significant increase in both CD4$^+$ and CD8$^+$ T cell in tumor tissue was found in the IT group compared with the CV group (IT *vs.* CV, P<0.001), and there was no obvious difference between regulatory T (Treg) cell percentage in the three groups (*Figure 16*). In peripheral blood, there was no statistically significant difference in the CD4$^+$, CD8$^+$, and Treg cell percentage between the three groups. Furthermore, we examined the immunosuppressive markers LAG-3, TIM-3, and PD-1; the three markers increased in the three groups at week 3, and the highest level was in the IT group (*Figure 17*). Under the decreased tumor burden conditions, the immunosuppressive markers increased.

Discussion

We took advantage of an orthotopic CRLM model to estimate two delivery routes of CAR T-cells to treat CRLM. MSLN was selected as a cell-surface antigen because of its overexpression in most gastrointestinal malignant tumors

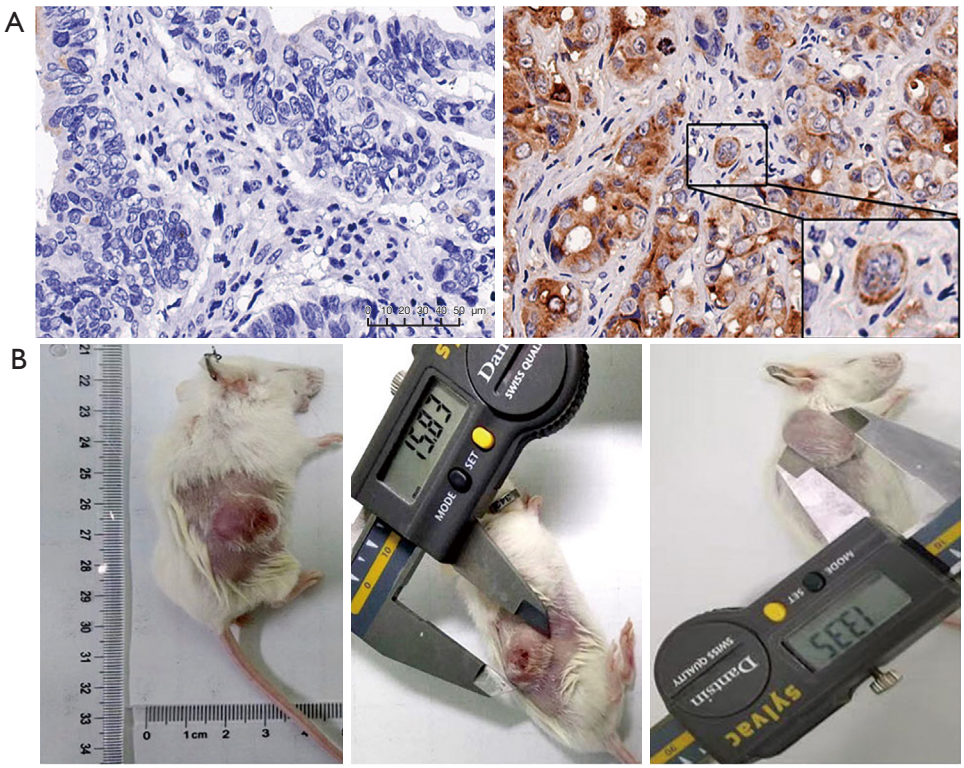

Figure 12 MSLN$^+$CRLM PDX mouse model establishment. (A) The IHC results of MSLN expression of CRLM (left, negative; right, strong positive, 20×, magnification to 40×); (B) CRLM PDX model. MSLN, mesothelin; CRLM, colon cancer liver metastasis; PDX, patient-derived xenograft; IHC, immunohistochemistry.

and correlation with cancer cell aggressiveness, invasion, and proliferation, and low expression in normal tissues (20,21). We demonstrated that PV delivery of CAR T-cells was superior to systemic delivery.

CAR T-cell therapy exhibits high efficiency but is limited by significant toxicity. Systemically delivered CAR T-cells are circulated in the lungs prior to tumor infiltration. The dose of systemic delivery is correlated with CAR T-cell antitumor effect, and as systemic doses increases, so does the risk of toxicity (22). Given this low therapeutic window, novel approaches are necessary to reduce systemic CAR T-cell concentrations. One method to avoid the circulating load of CAR T-cell in solid tumors might be regional delivery (23). In CRLM, research has shown that regional hepatic artery delivery of CAR T-cell to liver metastases outperformed systemic delivery (24). In our study, we selected an NSG mouse model with better compatibility between human MSLN CAR T-cells and human tumor cells. However, due to the difficulties of artery puncture in NSG mice and feeding difficulties in large immunodeficient animals, and considering the dual blood supply of hepatic artery and PV in liver tumors, the first-pass effect of drugs, and other factors, we delivered a single low-dose CAR T-cells via the PV, reducing the puncture risk and dose-dependent problems, and no interleukin was used. The results showed that PV administration of MSLN CAR T-cells could significantly inhibit CRLM tumor burden, and the efficacy was better than that of systemic administration. PV administration of MSLN CAR T-cell in the orthotopic CRLM mouse model was well tolerated, without obvious side effects to vital organs. The efficiency of CAR T-cell in solid tumors faces another important limitation impeded by the quality of T cells isolated from the donor. In our study, we found that low-transduced MSLN CAR T-cells became effective in the treatment of CRLM, partly due to PV administration. In previous research, most patients with metastatic liver cancer were already in the middle and late stages at diagnosis, and their systemic condition was poor (25). Regional administration is an ideal way to treat these patients, which can reduce the dosage, reduce the

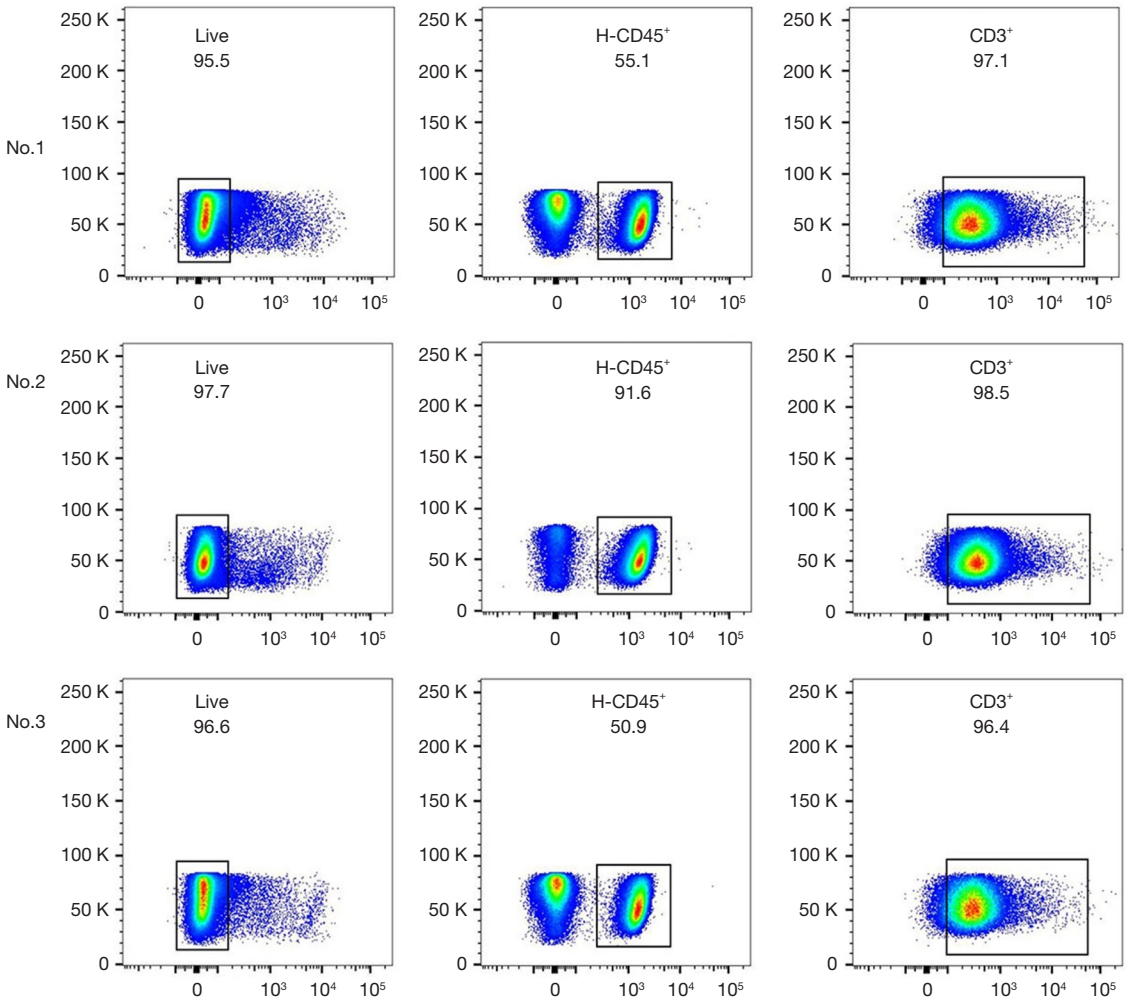

Figure 13 Human immune reconstitution mice model.

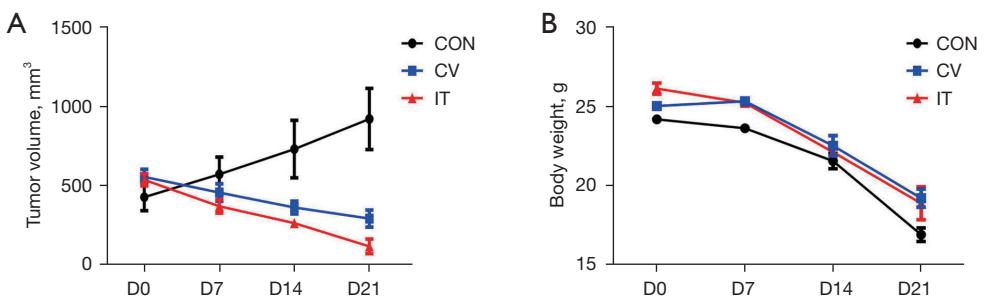

Figure 14 The body weight and survival curve of PDX model. CON, control; CV, caudal vein; IT, intratumor; PDX, patient-derived xenograft.

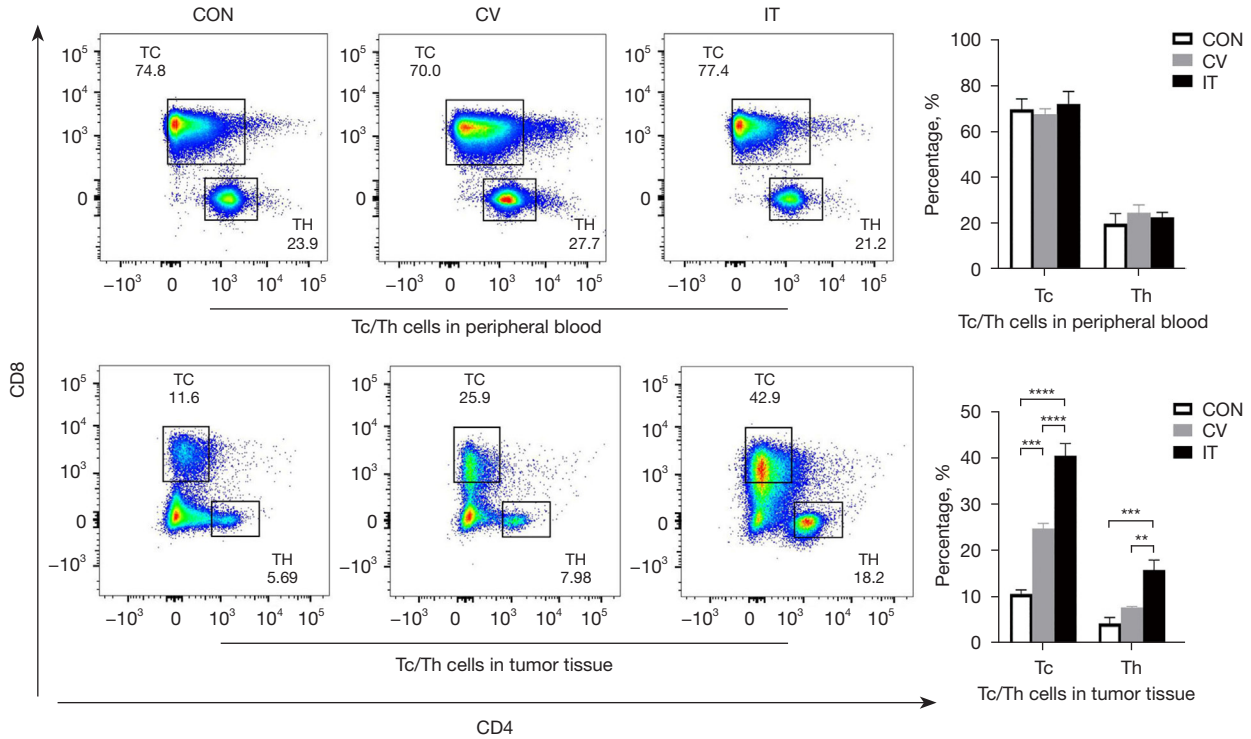

Figure 15 Tc/Th cells distribution in tumor tissue and peripheral blood. **, represents P<0.01; ***, represents P<0.001; ****, represents P<0.0001. CON, control; CV, caudal vein, IT, intratumor; Tc, cytotoxic T; Th, T helper.

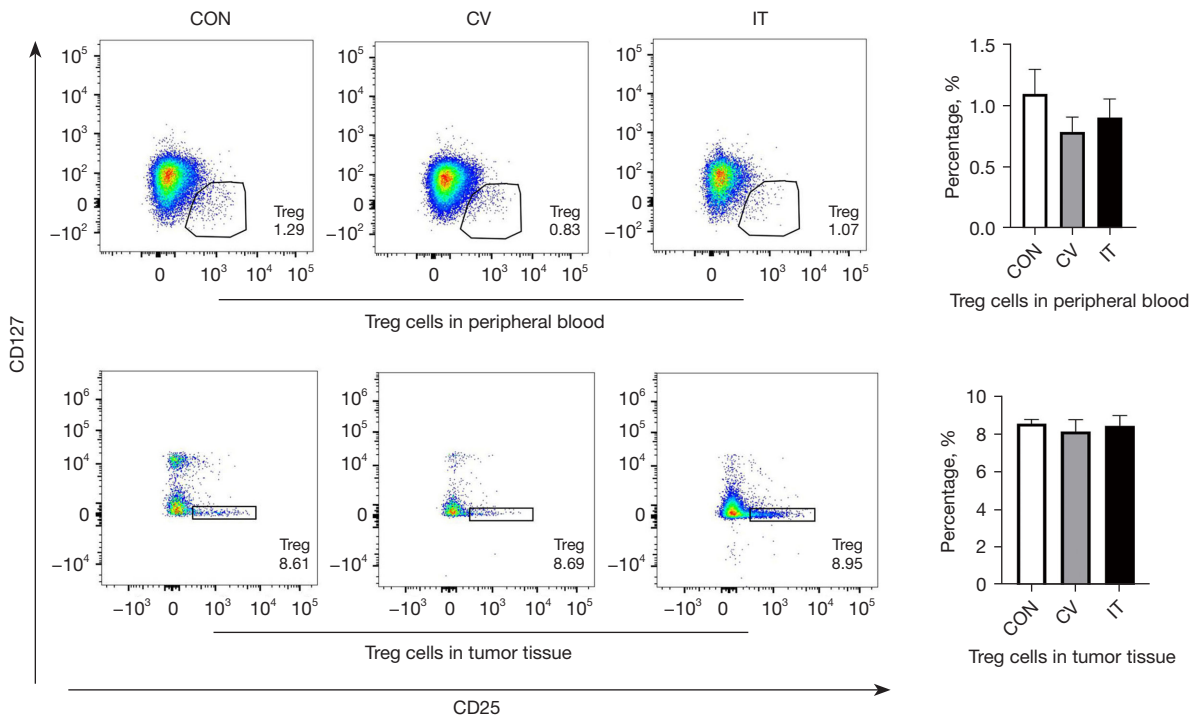

Figure 16 Treg cell distribution in tumor tissue and peripheral blood. CON, control; CV, caudal vein, IT, intratumor; Treg, regulatory T.

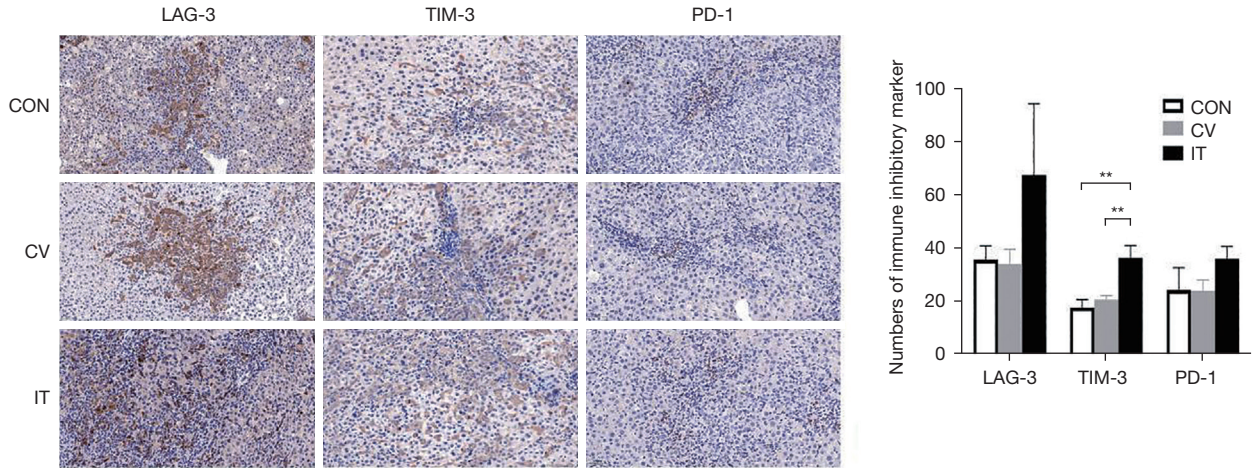

Figure 17 The IHC results of immunosuppressive marker expression in tumor tissue (10×). **, represents P<0.01. CON, control; CV, caudal vein; IT, intratumor; IHC, immunohistochemistry.

burden on normal organs, and reduce side effects.

The ineffective infiltration of CAR T-cell into solid tumors poses another obstacle to the clinical use of CAR T-cell for solid tumors (26,27). CAR T-cell infiltration, homing and amplification could persist killing tumor cells and stimulate cytokine secretion, to enhance the antitumor effect and modulate the immune microenvironment (28-30). In our study, the percentage of MSLN CAR T-cells in tumor tissue was much higher than that of systemic administration, and $CD8^+GB^+$ T cells were significantly increased in tumor tissue. The secretion of various cytokines increased, which enhanced the anti-tumor immune response. Regional administration of T cells was found to enhance CAR T-cell infiltration and persistence into the solid tumor. This result is consistent with the published literature, which has illustrated that CAR T-cell therapy combined with the immune checkpoint inhibitor can reverse the tumor microenvironment and increase the anti-tumor activity of T cells (19,31,32).

Finally, CAR T-cell exhaustion in solid tumor was due to tumor antigen stimulation and immunosuppressive tumor microenvironment. An immunosuppressive microenvironment has been shown to prevent the successful application of CAR T-cell to target CRLM (33,34). Katz *et al.* (24) evaluated transhepatic arterial injection of targeted carcinoembryonic antigen $(CEA)^+$ CAR T-cells for the treatment of patients with CRLM, and showed that local infusion could improve the tumor-killing effect of CAR T-cells, which was better than intravenous injection and limited the growth of systemic lesions. Due to the limitation of humanistic care and ethical issues about the regional administration of CAR T-cell for CRLM, no immune-relevant analysis was conducted.

We developed a human immune reconstruction and PDX model to mimic the real human immune environment of T cell. In the PDX model, IT administration and CV administration mainly changed the cytotoxic T (Tc) ($CD8^+$ T cell) and Th ($CD4^+$ T cell) percentage in tumor tissue, but did not affect Treg by the time the study had been terminated. The efficacy was better in the IT group compared with the CV group. This superior efficacy was dependent on regional administration of MSLN CAR T-cells infiltrated earlier into the tumor than systemic administration, resulted in earlier tumor antigen encounter, T-cell activation, cytokine secretion, $CD4^+$ and $CD8^+$ CAR T-cell proliferation and function (35). Regional administration of CAR T-cell not only enhanced the antitumor response, but also converted the cold tumor to a hot tumor. To our surprise, after 3 weeks of observation, although CAR T-cell was still discovered in tumor tissue, the killing effect weakened, and the level of immunosuppressive markers was elevated in IT group. This is consistent with the results reported in the literature (36,37) that when Tc cells performed the killing function, a variety of immune checkpoint molecules were up-regulated, including PD-1, PD-L1, CTLA4, LAG3, and IDO, which gradually led to functional exhaustion of activated T-cells. However, due to the limited observation time of the model, the influence trend in the later period is not clear.

Although the exhausted T cells exist in the tissue, they do not have an effective killing function, so even if the presence of T cells is detected, they do not necessarily have an anti-tumor function. This highlights that in the development of CAR T-cells, more attention should be paid to the "quality" of CAR T-cells to optimize them so that they can play a long-term killing role.

Conclusions

In summary, our study demonstrates the safety and efficacy of PV administration of MSLN CAR T-cell in the orthotopic CRLM NSG mouse model. Moreover, we preliminarily analyzed the change of tumor immune microenvironment after regional delivery of MSLN CAR T-cell in CRLM PDX mouse model. Our study revealed regional delivery of MSLN CAR T-cell may be a new therapeutic option for CRLM. Now, we are trying to improve CAR construct, and combine with other treatments, such as ^{125}I seeds implantation, microwave ablation, to improve antitumor effect of CAR T-cell therapy. Interventional treatment and CAR T-cell therapy combinations may be the future direction for CRLM treatment option.

Acknowledgments

Funding: This study was supported by the National Natural Science Foundation of China (No. 81771948).

Footnote

Reporting Checklist: The authors have completed the ARRIVE reporting checklist. Available at https://jgo.amegroups.com/article/view/10.21037/jgo-24-25/rc

Data Sharing Statement: Available at https://jgo.amegroups.com/article/view/10.21037/jgo-24-25/dss

Peer Review File: Available at https://jgo.amegroups.com/article/view/10.21037/jgo-24-25/prf

Conflicts of Interest: All authors have completed the ICMJE uniform disclosure form (available at https://jgo.amegroups.com/article/view/10.21037/jgo-24-25/coif). Jingwen Tan, N.X., and L.Y. are from Shanghai Unicar-Therapy Bio-Medicine Technology Co., Ltd., Shanghai, China. The other authors have no conflicts of interest to declare.

Ethical Statement: The authors are accountable for all aspects of the work in ensuring that questions related to the accuracy or integrity of any part of the work are appropriately investigated and resolved. Experiments were performed under a project license (No. B2020-009R2) granted by the Institutional Animal Care and Use Committee of Zhongshan Hospital, Fudan University and institutional guidelines for the care and use of animals were followed.

References

1. Tsilimigras DI, Brodt P, Clavien PA, et al. Liver metastases. Nat Rev Dis Primers 2021;7:27.
2. Luo Z, Bi X. Surgical treatment of colorectal cancer liver metastases: individualized comprehensive treatment makes a difference. Hepatobiliary Surg Nutr 2021;10:899-901.
3. Ruffolo LI, Hernandez-Alejandro R, Tomiyama K. Refining the surgical playbook for treating colorectal cancer liver metastases. Hepatobiliary Surg Nutr 2021;10:397-400.
4. Porter DL, Hwang WT, Frey NV, et al. Chimeric antigen receptor T cells persist and induce sustained remissions in relapsed refractory chronic lymphocytic leukemia. Sci Transl Med 2015;7:303ra139.
5. Adusumilli PS, Zauderer MG, Rivière I, et al. A Phase I Trial of Regional Mesothelin-Targeted CAR T-cell Therapy in Patients with Malignant Pleural Disease, in Combination with the Anti-PD-1 Agent Pembrolizumab. Cancer Discov 2021;11:2748-63.
6. Kreitman RJ, Hassan R, Fitzgerald DJ, et al. Phase I trial of continuous infusion anti-mesothelin recombinant immunotoxin SS1P. Clin Cancer Res 2009;15:5274-9.
7. Hollevoet K, Mason-Osann E, Liu XF, et al. In vitro and in vivo activity of the low-immunogenic antimesothelin immunotoxin RG7787 in pancreatic cancer. Mol Cancer Ther 2014;13:2040-9.
8. Le DT, Brockstedt DG, Nir-Paz R, et al. A live-attenuated

Listeria vaccine (ANZ-100) and a live-attenuated Listeria vaccine expressing mesothelin (CRS-207) for advanced cancers: phase I studies of safety and immune induction. Clin Cancer Res 2012;18:858-68.
9. Ordóñez NG. Application of mesothelin immunostaining in tumor diagnosis. Am J Surg Pathol 2003;27:1418-28.
10. Pastan I, Hassan R. Discovery of mesothelin and exploiting it as a target for immunotherapy. Cancer Res 2014;74:2907-12.
11. DeSelm CJ, Tano ZE, Varghese AM, et al. CAR T-cell therapy for pancreatic cancer. J Surg Oncol 2017;116:63-74.
12. Morello A, Sadelain M, Adusumilli PS. Mesothelin-Targeted CARs: Driving T Cells to Solid Tumors. Cancer Discov 2016;6:133-46.
13. Liu Y, He Y. A narrative review of chimeric antigen receptor-T (CAR-T) cell therapy for lung cancer. Ann Transl Med 2021;9:808.
14. Nellan A, Rota C, Majzner R, et al. Durable regression of Medulloblastoma after regional and intravenous delivery of anti-HER2 chimeric antigen receptor T cells. J Immunother Cancer 2018;6:30.
15. Katz SC, Point GR, Cunetta M, et al. Regional CAR-T cell infusions for peritoneal carcinomatosis are superior to systemic delivery. Cancer Gene Ther 2016;23:142-8.
16. Priceman SJ, Tilakawardane D, Jeang B, et al. Regional Delivery of Chimeric Antigen Receptor-Engineered T Cells Effectively Targets HER2(+) Breast Cancer Metastasis to the Brain. Clin Cancer Res 2018;24:95-105.
17. Shen X, Zhang R, Nie X, et al. 4-1BB Targeting Immunotherapy: Mechanism, Antibodies, and Chimeric Antigen Receptor T. Cancer Biother Radiopharm 2023;38:431-44.
18. Kang L, Zhang J, Li M, et al. Characterization of novel dual tandem CD19/BCMA chimeric antigen receptor T cells to potentially treat multiple myeloma. Biomark Res 2020;8:14.
19. Adusumilli PS, Cherkassky L, Villena-Vargas J, et al. Regional delivery of mesothelin-targeted CAR T cell therapy generates potent and long-lasting CD4-dependent tumor immunity. Sci Transl Med 2014;6:261ra151.
20. Servais EL, Colovos C, Rodriguez L, et al. Mesothelin overexpression promotes mesothelioma cell invasion and MMP-9 secretion in an orthotopic mouse model and in epithelioid pleural mesothelioma patients. Clin Cancer Res 2012;18:2478-89.
21. Jiang W, Gu G, Zhang Y, et al. Novel mesothelin-targeted chimeric antigen receptor-modified UNKT cells are highly effective in inhibiting tumor progression. Pharmacol Res 2023;197:106942.
22. Flugel CL, Majzner RG, Krenciute G, et al. Overcoming on-target, off-tumour toxicity of CAR T cell therapy for solid tumours. Nat Rev Clin Oncol 2023;20:49-62.
23. Li T, Luo R, Su L, et al. Advanced Materials and Delivery Systems for Enhancement of Chimeric Antigen Receptor Cells. Small Methods 2023;7:e2300880.
24. Katz SC, Burga RA, McCormack E, et al. Phase I Hepatic Immunotherapy for Metastases Study of Intra-Arterial Chimeric Antigen Receptor-Modified T-cell Therapy for CEA+ Liver Metastases. Clin Cancer Res 2015;21:3149-59.
25. Tomlinson JS, Jarnagin WR, DeMatteo RP, et al. Actual 10-year survival after resection of colorectal liver metastases defines cure. J Clin Oncol 2007;25:4575-80.
26. Liu S, Zhang Y. Challenges and interventions of chimeric antigen receptor-T cell therapy in solid tumors. Chin J Cancer Res 2023;35:239-44.
27. Zhai X, Mao L, Wu M, et al. Challenges of Anti-Mesothelin CAR-T-Cell Therapy. Cancers (Basel) 2023;15:1357.
28. Katz SC, Pillarisetty V, Bamboat ZM, et al. T cell infiltrate predicts long-term survival following resection of colorectal cancer liver metastases. Ann Surg Oncol 2009;16:2524-30.
29. Kalos M, Levine BL, Porter DL, et al. T cells with chimeric antigen receptors have potent antitumor effects and can establish memory in patients with advanced leukemia. Sci Transl Med 2011;3:95ra73.
30. Klobuch S, Seijkens TTP, Haanen JBAG. The emerging role for CAR T cells in solid tumor oncology. Chin Clin Oncol 2023;12:19.
31. Emtage PC, Lo AS, Gomes EM, et al. Second-generation anti-carcinoembryonic antigen designer T cells resist activation-induced cell death, proliferate on tumor contact, secrete cytokines, and exhibit superior antitumor activity in vivo: a preclinical evaluation. Clin Cancer Res 2008;14:8112-22.
32. Cherkassky L, Morello A, Villena-Vargas J, et al. Human CAR T cells with cell-intrinsic PD-1 checkpoint blockade resist tumor-mediated inhibition. J Clin Invest 2016;126:3130-44.
33. Katz SC, Bamboat ZM, Maker AV, et al. Regulatory T cell infiltration predicts outcome following resection of colorectal cancer liver metastases. Ann Surg Oncol 2013;20:946-55.
34. Yeku O, Li X, Brentjens RJ. Adoptive T-Cell Therapy

for Solid Tumors. Am Soc Clin Oncol Educ Book 2017;37:193-204.
35. Lanitis E, Poussin M, Hagemann IS, et al. Redirected antitumor activity of primary human lymphocytes transduced with a fully human anti-mesothelin chimeric receptor. Mol Ther 2012;20:633-43.
36. Eil R, Vodnala SK, Clever D, et al. Ionic immune suppression within the tumour microenvironment limits T cell effector function. Nature 2016;537:539-43.
37. Llosa NJ, Cruise M, Tam A, et al. The vigorous immune microenvironment of microsatellite instable colon cancer is balanced by multiple counter-inhibitory checkpoints. Cancer Discov 2015;5:43-51.

Cite this article as: Zhou X, Yang M, Yu J, Tan J, Xu N, Zhou Y, Zhang W, Ma J, Zhang Z, Friedlaender A, Taylor J, Yu L, Yan Z. Regional delivery of mesothelin-targeted chimeric antigen receptor T-cell effectively and safely targets colorectal cancer liver metastases in mice. J Gastrointest Oncol 2024;15(1):312-329. doi: 10.21037/jgo-24-25

